Research Square

Preprints are preliminary reports that have not undergone peer review.
They should not be considered conclusive, used to inform clinical practice,
or referenced by the media as validated information.

Optimizing IMS Coverage: Evaluating Esperanza, Belgrano II, and Neumayer III as Alternative Relocation Sites for the Antarctic Noble Gas Station

Hamed Abdollahnejad

h.abdollahnejad@umz.ac.ir

University of Mazandaran

Mohammad Sabzian

Amirkabir University of Technology

Research Article

Keywords: RN69 Relocation, ATM, Radioxenon, IMS network

Posted Date: March 2nd, 2026

DOI: https://doi.org/10.21203/rs.3.rs-8937595/v1

License: This work is licensed under a Creative Commons Attribution 4.0 International License.
Read Full License

Additional Declarations: No competing interests reported.

Abstract

The International Monitoring System for CTBT verification relies on noble-gas stations to detect atmospheric radioxenon. This study extends RN69 relocation analyses by evaluating Antarctic candidates Esperanza Belgrano II Neumayer III and Rotra to develop a comprehensive IMS deployment framework. Backward atmospheric transport modeling, source-receptor field analyses, and network-coverage assessments are applied to a hypothetical one-kiloton event with results computed daily and aggregated monthly and annually. The findings indicate Rotra and Esperanza are the largest contributors to network coverage, with mean values of approximately 0.80 percent and 0.76 percent, respectively. Esperanza offers greater spatial extent, about 33.44 percent compared with Rotra at 33.02 percent, and shorter periods of low coverage at 10% and 20% thresholds (8 vs 11 and 12 vs 14 days). Relocation gains are about 0.44 percent for Esperanza and 0.48 percent for Rotra, with smaller or mixed effects for the other sites and occasional reductions in the Eastern Hemisphere. The Consecutive Days Below Threshold metric highlights persistent vulnerabilities and complements average network coverage, guiding deployment decisions when combined with modeling and cost considerations.

1. Introduction

The International Monitoring System (IMS) under the Comprehensive Nuclear-Test-Ban Treaty (CTBT) relies on a global network of noble gas monitoring stations to detect atmospheric radioxenon isotopes, such as ^{133}Xe, ^{135}Xe, ^{131m}Xe and, ^{133m}Xe. These isotopes which serve as key signatures for verifying nuclear explosions (Kalinowski & Tatlisu, 2021) (Zähringer et al., 2009). Various sources contribute to the production and emission of these radioxenons into the atmosphere, resulting in a global background that varies among stations (Goodwin et al., 2021)(Topin et al., 2020). Consequently, in addition to the quality and precision of the equipment used at the stations (Cagniant et al., 2018)(Fritioff et al., 2017), this background can significantly affect the performance of all stations (Bowyer, 2021)(Bowyer et al., 2013). Furthermore, techniques based on isotopic ratio discrimination have been developed to distinguish nuclear tests from background emissions (Kalinowski et al., 2014)(Kalinowski et al., 2010).

However, the key factor influencing the overall efficiency and effectiveness of the network is the strategic placement of each station, which necessitates a review and optimization of the locations of specific inactive stations. In this context, studies utilizing atmospheric transport modeling have been conducted to evaluate its effect on the radioxenon network coverage (Abdollahnejad et al., 2022).

In remote regions like Antarctica, these stations are essential for ensuring comprehensive coverage of the southern hemisphere; however, their placement must balance detection sensitivity, logistical feasibility, and resilience to extreme environmental conditions. The Antarctic noble gas station at RN69, located at approximately 75°58’S, 26°73’W, encounters logistical challenges such as transportation difficulties and extreme weather, necessitating its relocation to enhance operational efficiency and data reliability. This situation underscores the need to identify alternative sites, requiring thorough

assessments of site suitability, environmental impacts, and detection capabilities throughout the relocation process.

Recent research has highlighted the potential benefits of repositioning the existing RN69 noble gas station to alternative sites such as Rothera and Troll to enhance detection sensitivity, mitigate logistical challenges, and improve overall IMS network efficiency (Abdollahnejad, 2025). This optimization is particularly relevant given the harsh Antarctic environment, where station placement can significantly affect data quality and operational costs. Previous assessments have demonstrated that strategic rearrangements can substantially enhance noble gas Network Coverage (NC), thereby strengthening global verification regimes.

Building on this foundational analysis by Abdollahnejad, the present study extends the comparative assessment by incorporating three additional Antarctic research stations—Esperanza, Belgrano II, and Neumayer III—as potential relocation candidates for RN69. These sites, located along the Antarctic Peninsula and the coast of the Weddell Sea, offer diverse geographical and climatic profiles that may help fill gaps in southern hemisphere radioxenon coverage. Through the assessment of these alternatives, the study yields a more comprehensive framework and presents the novel parameter Consecutive Days Below the Threshold as the principal innovation, informing the optimization of IMS station relocation decisions.

2. Materials and Methods

2.1. Network and proposed sites

The IMS radionuclide station network consists of 79 deployed stations, with 39 of them set to feature advanced measurement systems for radioxenons (Liu et al., 2023). The majority of these stations are currently operational and are transmitting updated data to the International Data Center (IDC) (Gadey, 2023).

The station number 69 in the noble gas network (RN69) has been proposed for replacement due to logistical challenges. This study employs a comparative modeling approach adapted from prior IMS optimization frameworks, focusing on geospatial, atmospheric, and logistical parameters to evaluate the potential relocation of the RN69 station. Building on previous analyses that considered Rothera and Troll as alternatives, this research further explores Esperanza, Belgrano II, and Neumayer III as viable options. These candidate sites were selected based on their operational status and geographical distribution across different sectors of Antarctica, allowing for a comprehensive assessment of their potential to enhance the monitoring capability of the network.

Esperanza Station, situated on the Antarctic Peninsula at roughly 63°40’S, 57°00’W, is operated by Argentina and stands 37 meters above sea level. It maintains a year-round staff and features robust infrastructure that facilitates diverse scientific research activities, positioning it as an excellent option for noble gas monitoring (Galindo-Zaldívar et al., 2013).

Belgrano II Station is located inland in East Antarctica at approximately 77°87’S, 34°63’W, and is operated by Argentina, standing at an elevation of 60 meters above sea level. Although it encounters logistical challenges due to its remote setting, it may potentially yield valuable data for noble gas monitoring due to its distinct atmospheric conditions (de Brito Neto et al., 2022).

Neumayer III Station is situated on the Ekström Ice Shelf at approximately 70°39’S, 8°16’W and is operated by Germany, with an elevation of 39 meters above sea level. This station operates year-round and is equipped with advanced facilities and an extensive weather monitoring system, positioning it well for numerous scientific studies and providing considerable potential to strengthen the IMS network (Bockelmann et al., 2022).

Furthermore, it is worth mentioning that Rothera and Troll were examined in a prior study, and their details are included here solely for the sake of comparison. Table 1 summarizes the sites under consideration, along with the Antarctica IMS noble gas station, providing their full names, abbreviations, coordinates, owner countries, and distances from the current station. Figure 1 illustrates the locations of the sites of interest, highlighted in blue, alongside the IMS noble gas stations, which are marked in black.

Table 1
Detailed information on the sites under investigation and RN69 noble gas station, including abbreviations, complete names, longitude, latitude, owner countries, and Distance from RN69.

Abbreviation Name	Complete Name	Longitude	Latitude	Owner Country	Distance from RN69 (km)
Hal69	Holley (RN69)	-26.73	-75.58	UK	-
Esper	Esperanza	-57.00	-63.40	Argentina	1756
Belgr	Belgrano II	-34.63	-77.87	Argentina	324
Neuma	Neumayer III	-8.16	-70.39	Germany	801
Troll*	Troll	+ 2.53	-72.01	Norway	977
Rotra*	Rothera	-68.12	-67.57	UK	1654

* Analyzed in (Abdollahnejad, 2025).

2.2. Modelling

Atmospheric Transport Modeling (ATM) is essential for interpreting radioxenon detections at IMS stations within the CTBT framework by simulating plume dispersion from potential sources under realistic meteorology and radioactive decay (De Meutter et al., 2017). Forward modeling is employed to project releases from assumed sources to IMS stations and to estimate arrival concentrations of key isotopes, with attention to the spatiotemporal evolution of the plume (Ringbom et al., 2021). Backward transport modeling is utilized to identify Potential Source Regions (PSRs) by tracing air parcels over approximately two weeks in conjunction with meteorological data (Becker et al., 2010). This approach yields Source-Receptor Sensitivity (SRS) fields that relate the detected concentrations to possible

sources (Ringbom et al., 2014). These fields constitute the foundation of the NC evaluation, and the methodology for their calculation has been described in a previous publication based on (Wotawa et al., 2003).

2.3. NC Calculations

Notwithstanding the comprehensive description of the NC calculation methodology in (Abdollahnejad, 2025), a concise overview is provided here. Initially, SRS fields were generated for each site using meteorological data from the European Centre for Medium-Range Weather Forecasts (ECMWF) at a spatial resolution of 0.5° × 0.5° and 3-hourly intervals over the full year 2023, employing the Lagrangian Particle Dispersion Model (FLEXPART) (Pisso et al., 2019). Subsequently, an NC analysis was conducted to evaluate the capability of the noble gas IMS network to detect the release of ^{133}Xe resulting from a hypothetical 1-kiloton nuclear explosion.

The detection probability was computed based on the total released activity, the SRS matrix, the radioactive decay constant, and the detection thresholds of the IMS stations. The station-specific detection thresholds were defined as the mean Abnormal Concentration Level (ACL) of ^{133}Xe at each active station during 2023.

NC was first evaluated without any station in Antarctica. Then, each proposed site and the current station were added to the network individually, and the calculations were repeated. The difference between these cases quantifies the impact of each site on NC. These results were computed for each grid cell on a daily basis, with monthly and annual values obtained by averaging over the corresponding days, and are presented in Sections 3.1, 3.2 and 3.3.

Furthermore, the relocation effect was quantified by differencing the coverage obtained with activation of the sites under study and that produced by Hal69 (Section 3.4). The calculation and visualization methods for the NC analysis and data analysis sections are described in detail in the previous paper.

The Consecutive Days Below the Threshold metric quantifies the duration of sustained low network coverage across grids (Section 3.5). Higher values indicate persistent monitoring gaps, while lower values reflect greater network resilience. This metric complements average coverage by emphasizing the persistence, rather than severity, of coverage deficiencies.

3. Results and discussion

3.1. Annual Spatial Influence

Daily assessments were conducted to quantify the contribution of each of the five monitoring sites to the overall NC. Although the site-by-site influence fluctuates markedly from day to day, the overarching pattern illustrates a minimum impact from May to September, with a larger influence observed in January and December. Year-long averages reveal that Rotra and Esper have the largest effects on

improving the NC of the radioxenons stations capability, at 0.80% and 0.76% respectively. Belgr and Hal69 follow with 0.35% and 0.32%, while Neuma and Troll exhibit the smallest influence at 0.30% and 0.15%.

Figure 2 presents the annual mean zones of influence for each site. Blue areas indicate low influence, whereas red regions highlight areas with the greatest coverage gains. Given the close proximity of Rotra and Esper, their peak influence occurs in similar longitude bands, roughly between 15°E and 15°W and between 120°W and 5°E. Rotra reaches its maximum influence at (140.5°W, 80°S) with 14.00%, while Esper peaks at (139°W, 80°S) with 13.01%. In contrast, Hal69, Belgr, and Neuma attain their strongest influence in latitudinal ranges from 20°W to 10°E, with values of 11.32%, 11.06%, and 6.89% respectively. Troll, despite having the lowest average coverage, shows its greatest impact in the eastern hemisphere in the region from 0°W to 60°E, peaking at 4.14% at (3°E, 72.5°S).

3.1.1. Comparison of Rotra and Esper

Given that Rotra and Esper produced the largest positive impact on NC, a more detailed comparison of these two sites across latitude was performed. Latitudes from − 90° to -60° were averaged in 10° steps and plotted across longitudes; the results are represented in Fig. 3, with Rotra depicted by solid lines and Esper by dashed lines. The general trend shows Rotra's relative advantage across most longitudes, while Esper performs better than Rotra in longitudes between − 140° and − 110°, and this superiority is more pronounced at latitudes between − 80° and − 70°.

Furthermore, the enhancement of NC is predominantly concentrated in the western hemisphere for all examined latitudes. For both sites, the latitudinal band − 80° to -70° is colored red, indicating the highest influence across most regions; conversely, values in longitudes between 60°E and 120°E reach a minimum and have little impact on coverage. The blue shading indicates a sharp decrease at latitudes from − 70° to -60°, within the longitude range of 5°W to 60°E. Such a pronounced dip near the pole (black) has not been observed. Finally, For all scenarios, the peak values are observed at the boundary longitudes, namely the leftmost and rightmost ends of the longitude axis.

3.2. Monthly Assessment

An analysis of the monthly mean values of site-activation influence on NC is shown in the left panel of Fig. 4. The bars are color-coded as follows: orange for Troll, purple for Esper, green for Rotra, blue for Neuma, red for Belgr, and gray for Hal69. The findings demonstrate that in December, all five sites yield the greatest gains in coverage, with Troll achieving no more than a 1% increase, whereas the remaining sites exceed this threshold. In September, the sites represent the smallest impact on overall NC, with all effects falling under 1%.

In addition, the plot indicates that Esper and Rotra consistently register higher values than the other sites. A direct comparison reveals that Esper outperforms Rotra in April, June, September, and December, while in all other months (except March, where the values are equal) Rotra is higher. The top

end of the y-axis in the chart of annual mean impact on NC reflects these values, which were numerically analyzed in the previous section.

The next step involved analyzing the extent of coverage using the metric “percentage of grid cells covered at least once,” shown in the right panel of Fig. 4. The results show that the smallest geographic extent occurs in September for all sites. Regarding the maximum extent, the results are not clearly tied to a single NC magnitude. However, for this metric too, Rotra and Esper display higher values than the others in different months. Esper covers larger areas in February, March, April, June, and September, whereas Rotra leads in the other months.

The top portion of the chart presents the annual mean percentage of grid cells that have been covered at least once. This metric captures the annual fraction of coordinates that experienced any monitoring capability. The observed values are: Troll 33.60%, Esper 33.44%, Rotra 33.02%, Neuma 31.70%, Belgr 31.26%, and Hal69 30.88%. Although Troll has the weakest performance in magnitude of NC, it achieves the highest value on the current metric. In contrast to the previous metric, Esper demonstrates greater geographic extent than Rotra.

The year-long analysis also indicates that, although Esper trails Rotra slightly in total coverage by about 0.04 percentage points, it encompasses larger areas by roughly 0.42 percentage points. This suggests that Esper could be regarded as a serious option for relocating the RN69 station, pending more detailed investigations.

3.3. Rotra vs Esper: a daily comparison

The monthly analysis underscores the need for a closer examination of Rotra and Esper, with both metrics “magnitude of coverage” and “extent of coverage” being assessed daily. Figure 5 displays: (i) the daily difference in the NC amount (solid line) and (ii) the difference in the extent of coverage in favor of Esper over Rotra (dashed line). Positive values denote Esper’s lead; negative values denote Rotra’s lead. The greatest fluctuations for both metrics occur in January, February, November, and December, while the other months show more similar performance. The variation in geographic extent is greater than the variation in the amount of coverage, which remains relatively uniform.

Esper surpasses Rotra on 132 days for magnitude of coverage and on 163 days for extent of coverage, while Rotra leads on 181 and 194 days, respectively. Hence, although Rotra’s annual extent of coverage is lower, it achieves better performance on a larger number of days in daily comparisons. This suggests that on days when Esper expands coverage more than its competitors, its advantage strengthens, potentially boosting its annual average in its favor.

The highest relative advantage of Esper over Rotra in terms of coverage amount occurred on December 27, when Esper achieved 1.46 percentage more capability (Fig. 6, top row). In contrast, Rotra led by 2.27 percentage on January 2 (Fig. 6, bottom row). Regarding the extent of coverage, Esper covered 2.99 percentage more grid cells on February 19, its best performance in this metric; Rotra’s greatest extent advantage occurred on November 25, with 4.47 percentage more extent.

These results indicate substantial daily fluctuations over the year, with Esper outperforming on some days and Rotra on others. Since neither site consistently outperforms the other, a simple annual average gives a coarse summary and should not be treated as evidence of overall superiority.

3.4. The relocation impact

The impact of shifting the station from Hal69 to a new location across different coordinates is a crucial parameter for assessing the relocation's merits and drawbacks. For each grid cell, the result can be obtained by taking the daily difference between the current station being active and the presence of the new site. These daily calculations were carried out for all days, and the annual-average results for moving to the Neuma, Esper, Belgr, and Rotra stations are shown in Fig. 7. Hal69 and the sites under study are emphasized in bold on the maps, whereas the remaining network stations are depicted in normal weight. Yellow and red indicate zones in which relocation boosts NC, blue shades specify regions in which the current station outperforms and replacement would reduce its capability, and green denotes zones with negligible changes.

The bottom-right panel illustrates the relocation outcome to Belgr. The map is largely green, with only faint yellow shading in the western areas, signifying a negligible impact on total NC.

The bottom-left panel represents the repositioning to Neuma, showing many green zones and little to no effect. Nevertheless, a blue band spanning 30°W to 20°E suggests that Hal69 performs better there, implying that this moving would reduce capability in the specified polar region.

The upper-right panel displays the relocation outcome for moving the current station to Esper. In the longitudes from 30°W to 120°E, colored in light to dark blue, the transfer reduces NC, while elsewhere it enhances network performance. The gain in coverage is most evident in regions between 170°E and 120°W, highlighted in red.

The upper-left panel, depicting the replacement to Rotra, is shown to be highly similar to the Esper map; detailed results are reported in (Abdollahnejad, 2025). A direct comparison with Esper indicates that the positive values are somewhat larger at the listed longitudes (170°E – 120°W), resulting in more pronounced red regions. Moreover, the relocation results to Troll are presented in the preceding paper; owing to Troll's relatively poor performance in this analysis, no further commentary is offered.

Overall, the results demonstrate that displacing to Esper and Rotra increases capability across large portions of the Western Hemisphere, but there is a non-negligible decrease in coverage in the Eastern Hemisphere of the Antarctic. The spatial analysis of the repositioning outcomes shows that each relocation, despite improving coverage in some regions, leads to reduced coverage in other regions, and no sites provides better performance across all areas.

To obtain a more precise quantitative assessment, results were computed as monthly averages and grouped accordingly; Fig. 8 presents these results. The color coding for the sites follows Fig. 6. The y-axis shows monthly values as well as the annual mean for each relocation. The x-axis reflects the

magnitude of the impact, where negative values denote capability degradation and positive values denote gains.

As in the prior study Troll yields negative values in ten months reducing coverage. The annual average is a decrease of 0.16%. Neuma displays a somewhat better profile: negative values in six months, zeros in three months, and positive numbers in January and March (0.1 and 0.02). The annual-average change for Neuma is a slight decrease of 0.02%.

Given Belgr's closeness to the existing station, its behavior is largely comparable to that of the current location, and repositioning to this site does not produce substantial deviations. The moving to Belgr is characterized by three months of negative impact, three months with no impact, and the rest with minor improvements; the overall annual-average effect is a 0.03% increase in capability.

The relocation to Esper produces positive values throughout the year, ranging from 0.03% in June to over 1% in January, February, and December. The annual-average results indicate an overall 0.44% gain in NC.

According to previous paper, moving to Rotra increases the annual-average NC by 0.48%. The month-by-month comparison with Esper reveals equal performance in March; Esper leads in April, June, September, and December, whereas Rotra leads in the other months. Furthermore, day-by-day analyses show Rotra improves coverage on 305 days and Esper on 300 days, producing a minor overall annual advantage for Rotra of about 0.04%.

3.5. Consecutive Days Below the Threshold

The novel parameter, Consecutive Days Below the Threshold, was evaluated for its significance. It is defined as the number of consecutive days during which the total NC (including all noble gas stations) remains below the 10%, 20%, and 30% thresholds at each grid cell. Larger values indicate sustained network underperformance and larger monitoring gaps, whereas lower values reflect shorter and less frequent periods of underperformance, indicating greater network resilience. This metric captures the persistence of low-coverage episodes rather than their severity and therefore complements average coverage measures by highlighting persistent vulnerabilities. The results are presented in Table 2.

At the 10% threshold the six sites demonstrate 8 to 15 consecutive days below the threshold: Esper 8, Belgr 11, Hal69 11, Rotra 11, Neuma 11, Troll 15. The findings indicate that Troll exhibits the longest uninterrupted period of low coverage and that Esper exhibits the shortest, with the remaining alternative sites displaying comparable resilience to low-coverage events. The fact that Esper records 8 days versus Rotra's 11 days confirms that Esper experiences a shorter continuous-gap period and is less vulnerable to very low-coverage events at this threshold.

At the 20% threshold, Esper shows the shortest gap of 12 days, followed by Belgr and Hal69 at 13 days, Neuma and Rotra at 14 days, and Troll 18 days. This ranking is similar to that observed at the 10% threshold with Esper the shortest and Troll the longest. Escalating thresholds from 10% to 20%

demonstrates that more permissive thresholds prolong low-coverage episodes across sites, with Esper still exhibiting greater performance than Rotra.

At the 30% threshold, Hal69 and Belgr achieve the best result with 13 days, followed by Esper and Rotra at 14 days, Neuma at 15 days, and Troll at 20 days as the weakest. Equal durations for Esper and Rotra suggest that raising the acceptable-coverage threshold yields two sites with similar endurance, while Troll remains the most vulnerable with the longest gap. This pattern indicates that higher thresholds produce larger gaps across sites, and Belgr and Hal69 exhibit the strongest performance among them.

Table 2
The days on which NC remained continual below the threshold for the entire period.

site	Threshold (%)			
	10	20	30	
Esper	8	12	14	**Consecutive Days**
Belgr	11	13	13	
Hal69	11	13	13	
Rotra	11	14	14	
Neuma	11	14	15	
Troll	15	18	20	

4. Summary and Conclusions

This study compared five monitoring sites (Rotra, Esper, Troll, Belgr, Hal69, Neuma) across annual spatial influence, monthly activation, daily NC comparisons, relocation impacts, and the new metric of Consecutive Days Below the Threshold. The overall message is that Rotra and Esper each excel on different dimensions of network performance. Rotra provides the largest average improvement in NC (mean influence about 0.80%), with Esper close behind (0.76%). Belgr, Hal69, Neuma, and Troll show progressively smaller influences. This establishes Rotra as the strongest contributor to the magnitude of daily NC, on average.

However, Esper demonstrates a distinctly favorable profile when considering spatial extent and persistence of low-coverage episodes. In the annual extent metric (the percent of grid cells covered at least once), Esper attains a marginal but meaningful edge over Rotra (33.44% vs. 33.02%). Across months, Esper covers larger areas than Rotra in several periods (notably February, March, April, June, and September), while Rotra leads in other months. Collectively, these results imply that Esper provides broader geographic reach, despite Rotra’s higher per-day coverage contribution.

The Consecutive Days Below the Threshold results further reinforce Esper's stronger resilience. At the 10% threshold, Troll exhibits the longest uninterrupted low-coverage period, while Esper records the shortest (8 days vs. Rotra's 11 days). At 20%, Esper again shows the shorter gap (12 days) compared with Rotra (14 days). At 30%, Esper and Rotra are tied (14 days), with Troll remaining the outlier (20 days). Taken together, Esper sustains shorter runs of low coverage than Rotra across the lower thresholds and remains competitive at the highest threshold. This pattern points to greater persistence resilience for Esper.

Putting these strands together, Rotra is superior in terms of the magnitude of coverage it adds to the network on a daily basis, whereas Esper delivers broader spatial extent and fewer consecutive days with subthreshold performance. In other words, Rotra enhances how much coverage you get, while Esper expands the geographic footprint and maintains above-threshold performance more consistently over time.

These conclusions reinforce that relying solely on annual, monthly, or daily average metrics cannot fully characterize a station's contribution to the network's performance. Average measures can obscure important differences in where coverage exists and how persistently a station experiences periods of low availability, both of which are crucial for robust monitoring. Our findings indicate that a station may exhibit strong average NC yet leave large areas uncovered or undergo recurrent long gaps, while other sites may deliver broader geographic reach and greater temporal stability.

Consequently, it is essential to study and integrate new metrics such as the extent of coverage (the share of grid cells that experience coverage at least once) and Consecutive Days Below the Threshold into decision-making about deployment, relocation, and network optimization. Incorporating these metrics alongside dynamic atmospheric modeling, inter-site coordination, and practical considerations like feasibility and cost will yield a more reliable assessment of network capability.

Declarations

Author Contribution

H.A. originated the study, established the methodology, and directed the project; M.S. undertook the analyses and authored the manuscript. All authors reviewed and approved the final version of the manuscript.

Acknowledgement

The authors wish to convey their appreciation to the Iranian Radionuclide Laboratory (IRL) at Amir-Kabir University of Technology for their assistance and for granting access to IMS network data.

Disclaimer

The conclusions drawn in this study are the authors' and do not imply the official policy of any affiliated organization.

References

1. Abdollahnejad, H. (2025). Optimizing IMS Coverage: A Comparative Assessment of Relocating the Antarctic Noble Gas Station to Rothera and Troll: H. Abdollahnejad. *Pure and Applied Geophysics*, 1–14.
2. Abdollahnejad, H., Ochbelagh, D. R., & Azadi, M. (2022). Impact of the noble gas system NEX48 in Niger on the radioxenon global network coverage for the International Monitoring System of the comprehensive nuclear-test-ban treaty. *Journal of Environmental Radioactivity*, *250*, 106913.
3. Becker, A., Wotawa, G., Ringbom, A., & Saey, P. R. J. (2010). Backtracking of noble gas measurements taken in the aftermath of the announced October 2006 event in North Korea by means of PTS methods in nuclear source estimation and reconstruction. *Pure and Applied Geophysics*, *167*(4–5), 581–599.
4. Bockelmann, F., Dreier, A.-K., Zimmermann, J., & Peter, M. (2022). Renewable energy in Antarctica-photovoltaic for Neumayer Station III. *Solar Energy Advances*, *2*, 100026.
5. Bowyer, T. W. (2021). A review of global radioxenon background research and issues. *Pure and Applied Geophysics*, *178*, 2665–2675.
6. Bowyer, T. W., Kephart, R., Eslinger, P. W., Friese, J. I., Miley, H. S., & Saey, P. R. J. (2013). Maximum reasonable radioxenon releases from medical isotope production facilities and their effect on monitoring nuclear explosions. *Journal of Environmental Radioactivity*, *115*, 192–200.
7. Cagniant, A., Topin, S., Le Petit, G., Gross, P., Delaune, O., Philippe, T., & Douysset, G. (2018). SPALAX NG: A breakthrough in radioxenon field measurement. *Applied Radiation and Isotopes*, *134*, 461–465.
8. de Brito Neto, F. A., Mendes, D., & Spyrides, M. H. C. (2022). Analysis of extreme wind events in the Weddell Sea region (Antarctica) at Belgrano II Station. *Journal of South American Earth Sciences*, *116*, 103804.
9. De Meutter, P., Camps, J., Delcloo, A., & Termonia, P. (2017). Assessment of the announced North Korean nuclear test using long-range atmospheric transport and dispersion modelling. *Scientific Reports*, *7*(1), 1–9.
10. Fritioff, T., Axelsson, A., Mo¨rtsell, A., & & Ringbom, A. (2017). *SAUNA III new beta detector.* https://ctnw.ctbto.org/%0ADMZ/abstract/21821. Accessed 15 Sept 2019.
11. Gadey, H. R. (2023). Radioxenon Detection for Monitoring Subsurface Nuclear Explosion. In *Gamma Ray Imaging: Technology and Applications* (pp. 137–163). Springer.
12. Galindo-Zaldívar, J., Ruiz-Constán, A., Pedrera, A., Ghidella, M., Montes, M., Nozal, F., & Rodríguez-Fernandez, L. R. (2013). Magnetic anomalies in Bahia Esperanza: A window of magmatic arc

intrusions and glacier erosion over the northeastern Antarctic Peninsula. *Tectonophysics*, *585*, 68–76.

13. Goodwin, M. A., Davies, A. V, & Britton, R. (2021). Analysis of environmental radioxenon detections in the UK. *Journal of Environmental Radioactivity*, *234*, 106629.
14. Kalinowski, M. B., Axelsson, A., Bean, M., Blanchard, X., Bowyer, T. W., Brachet, G., Hebel, S., McIntyre, J. I., Peters, J., & Pistner, C. (2010). Discrimination of nuclear explosions against civilian sources based on atmospheric xenon isotopic activity ratios. *Pure and Applied Geophysics*, *167*(4–5), 517–539.
15. Kalinowski, M. B., Liao, Y.-Y., & Pistner, C. (2014). Discrimination of nuclear explosions against civilian sources based on atmospheric radioiodine isotopic activity ratios. *Pure and Applied Geophysics*, *171*(3–5), 669–676.
16. Kalinowski, M. B., & Tatlisu, H. (2021). Global radioxenon emission inventory from nuclear power plants for the calendar year 2014. *Pure and Applied Geophysics*, *178*(7), 2695–2708.
17. Liu, B., Kalinowski, M., Sun, Y., Carrigan, C. R., Saragiotis, C., Wang, J., Ertl, M., Kijima, Y., Schoemaker, R., & Kuśmierczyk-Michulec, J. (2023). Characterization of CTBT-relevant radioxenon detections at IMS stations using isotopic activity ratio analysis. *Pure and Applied Geophysics*, *180*(4), 1521–1540.
18. Pisso, I., Sollum, E., Grythe, H., Kristiansen, N. I., Cassiani, M., Eckhardt, S., Arnold, D., Morton, D., Thompson, R. L., & Groot Zwaaftink, C. D. (2019). The Lagrangian particle dispersion model FLEXPART version 10.4. *Geoscientific Model Development*, *12*(12), 4955–4997.
19. Ringbom, A., Axelsson, A., Aldener, M., Auer, M., Bowyer, T. W., Fritioff, T., Hoffman, I., Khrustalev, K., Nikkinen, M., & Popov, V. (2014). Radioxenon detections in the CTBT international monitoring system likely related to the announced nuclear test in North Korea on February 12, 2013. *Journal of Environmental Radioactivity*, *128*, 47–63.
20. Ringbom, A., Axelsson, A., Björnham, O., Brännström, N., Fritioff, T., Grahn, H., Hennigor, S., & Olsson, M. (2021). Radioxenon Releases from A Nuclear Power Plant: Stack Data and Atmospheric Measurements. *Pure and Applied Geophysics*, *178*(7), 2677–2693. https://doi.org/10.1007/s00024-020-02425-z
21. Topin, S., Gross, P., Achim, P., Generoso, S., Cagniant, A., Delaune, O., Morin, M., Philippe, T., Fontaine, J.-P., & Moulin, C. (2020). 6 months of radioxenon detection in western Europe with the SPALAX-New generation system-Part1: Metrological capabilities. *Journal of Environmental Radioactivity*, *225*, 106442.
22. Wotawa, G., De Geer, L.-E., Denier, P., Kalinowski, M., Toivonen, H., D'Amours, R., Desiato, F., Issartel, J.-P., Langer, M., & Seibert, P. (2003). Atmospheric transport modelling in support of CTBT verification—Overview and basic concepts. *Atmospheric Environment*, *37*(18), 2529–2537.
23. Zähringer, M., Becker, A., Nikkinen, M., Saey, P., & Wotawa, G. (2009). CTBT radioxenon monitoring for verification: today's challenges. *Journal of Radioanalytical and Nuclear Chemistry*, *282*(3), 737–742.

Figures

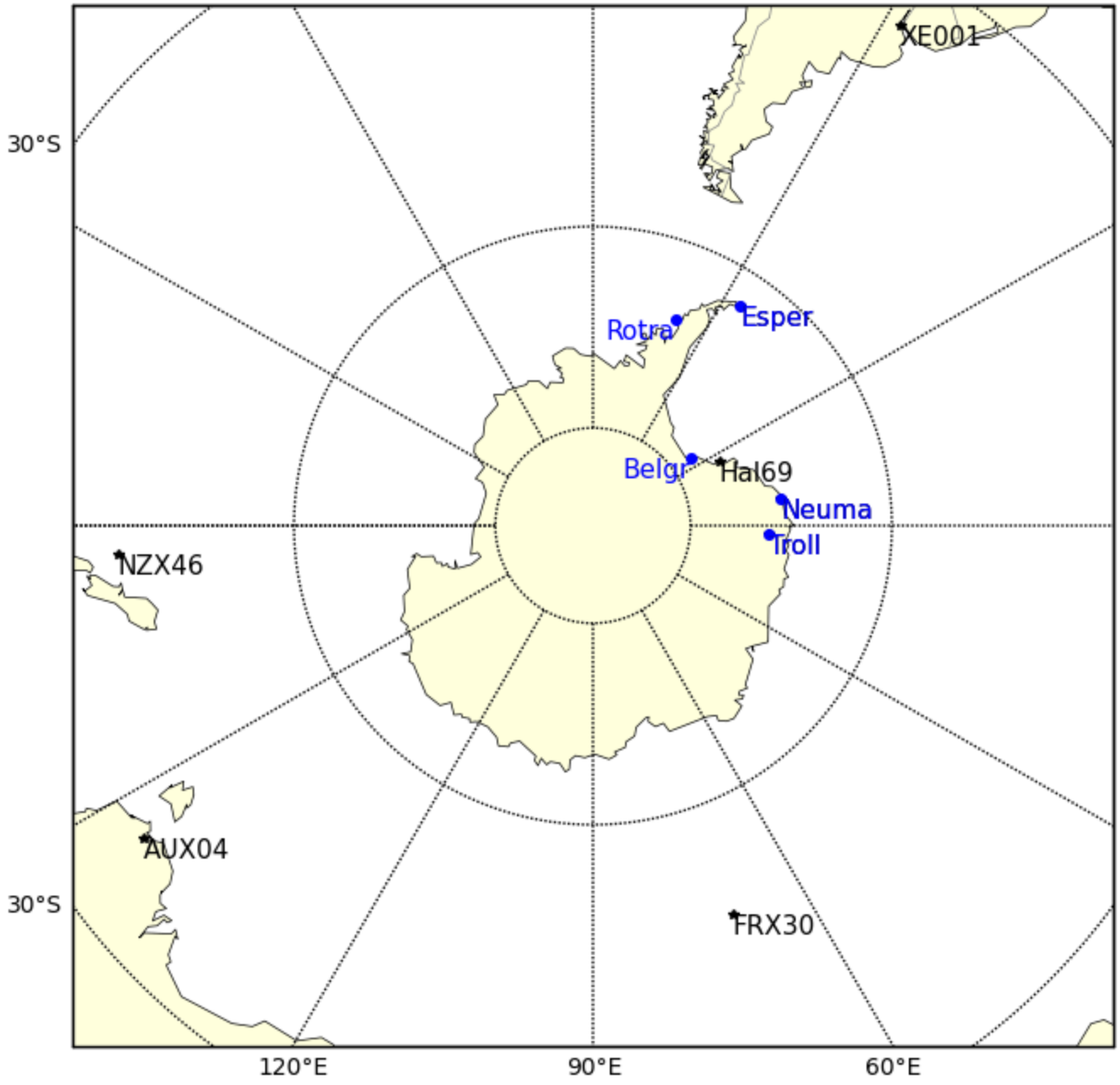


Figure 1

IMS noble gas stations (black) and sites currently being evaluated (blue).

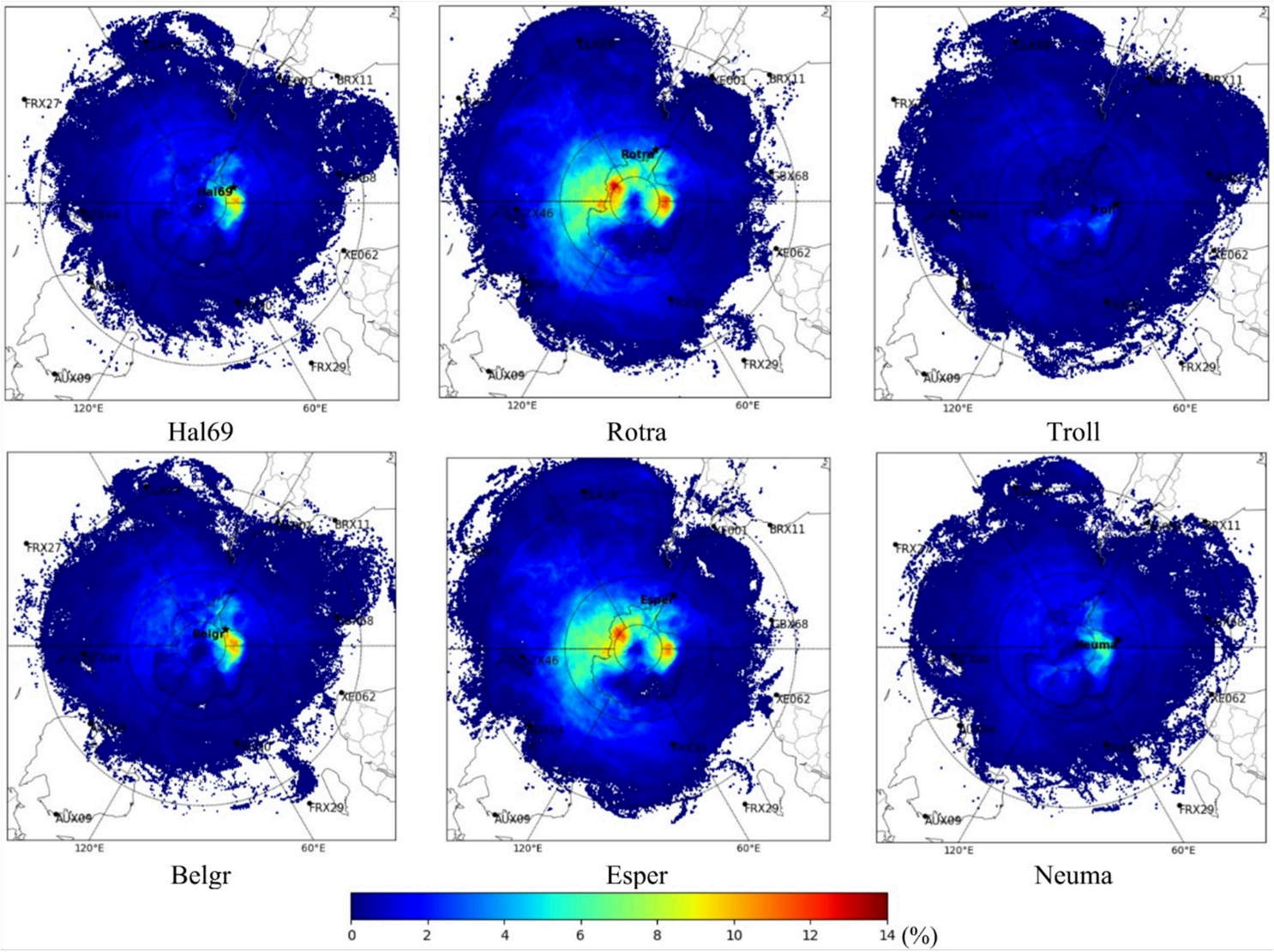


Figure 2

An average spatial influence on NC is observed across the year for the five investigated sites. The results for the first row were reported in the prior study (Abdollahnejad, 2025).

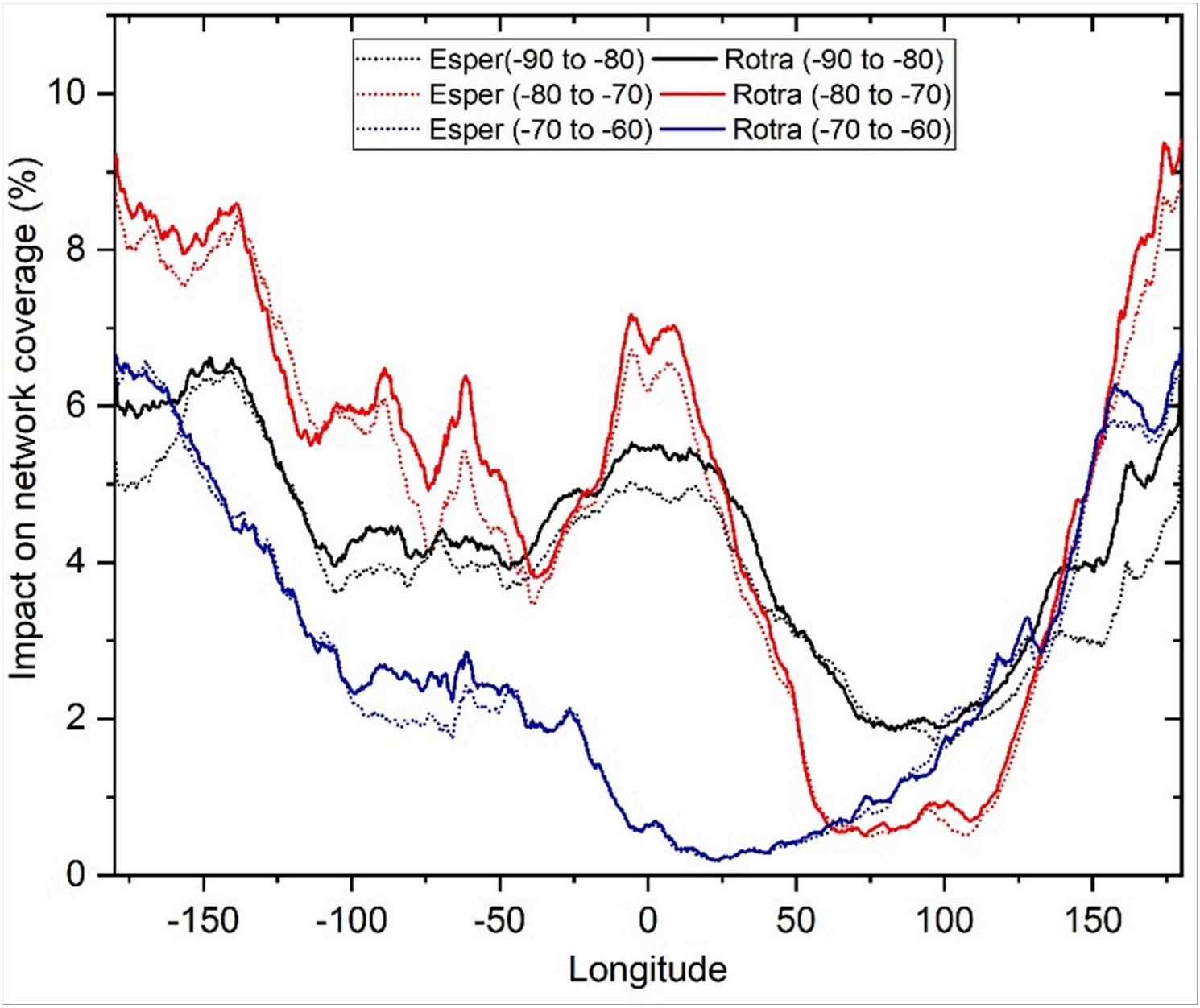


Figure 3

the comparative impact of Rotra and Esper on NC across longitudes for latitude bands -90° to -80° (black), -80° to -70° (red), and -70° to -60° (blue), with Rotra depicted by solid lines and Esper by dashed lines.

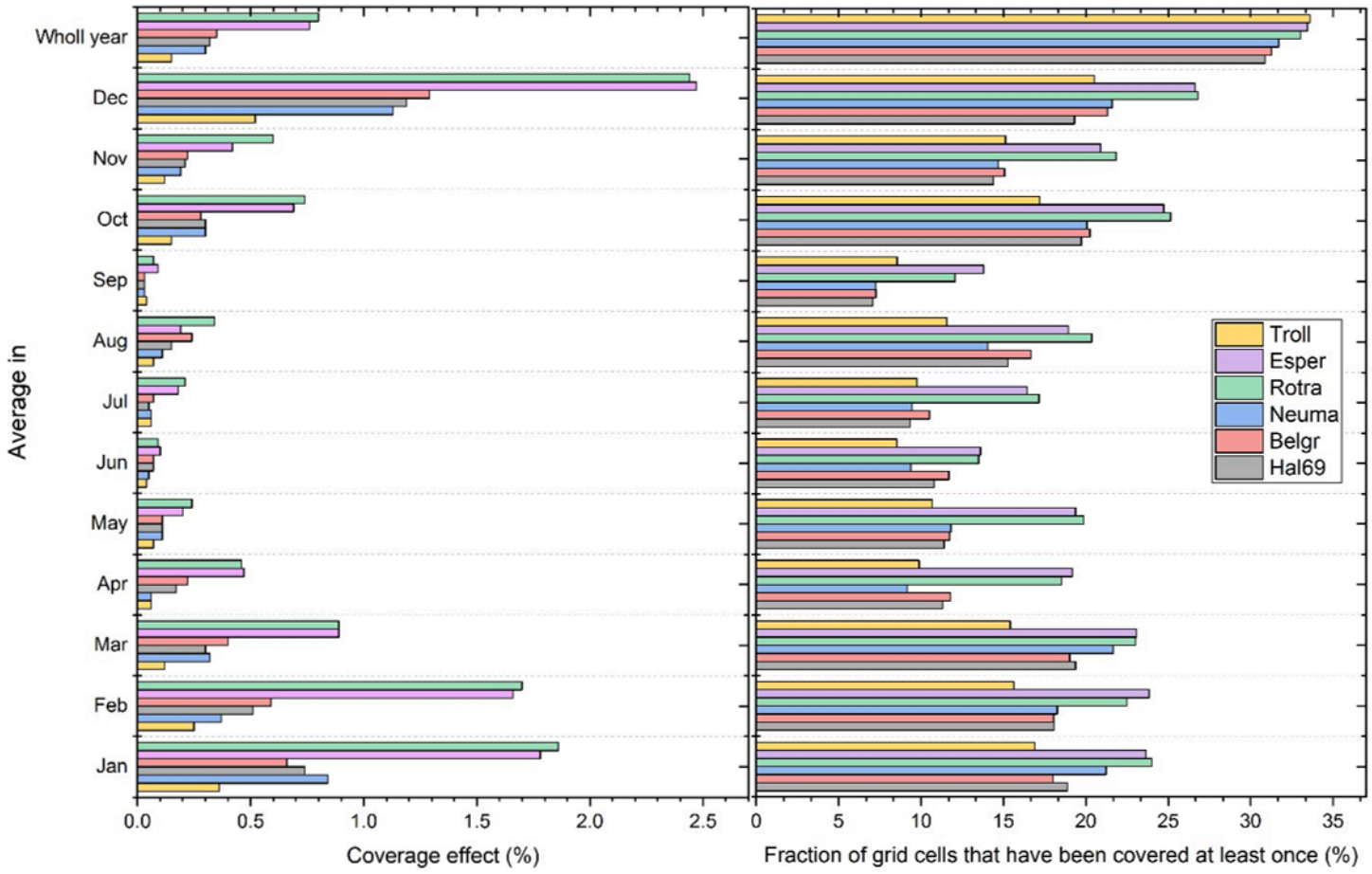


Figure 4

The left plot depicts the monthly average NC contributed by the five sites, and the right plot presents the proportion of grid cells that were covered at least once. Color correspond to sites: Troll (orange), Esper (purple), Rotra (green), Neuma (blue), Belgr (red), Hal69 (gray).

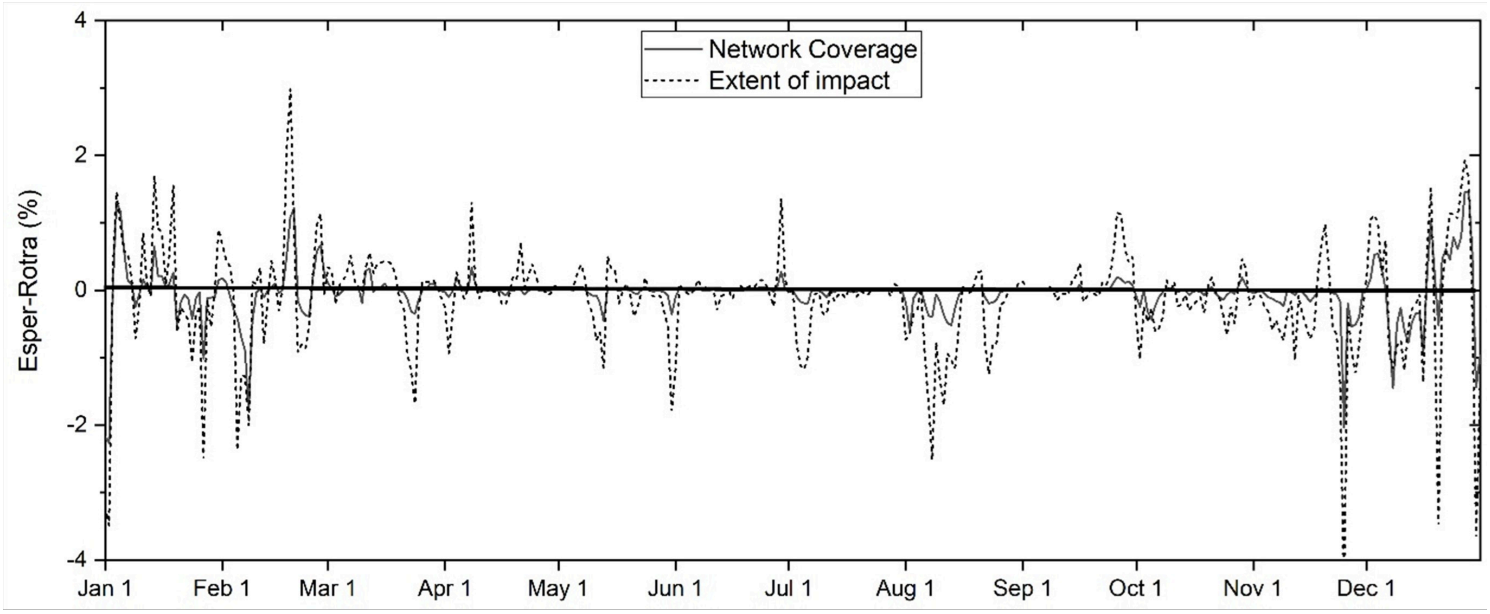


Figure 5

The difference between Esper and Rotra on NC (solid line) and on the extent of coverage (dashed line).

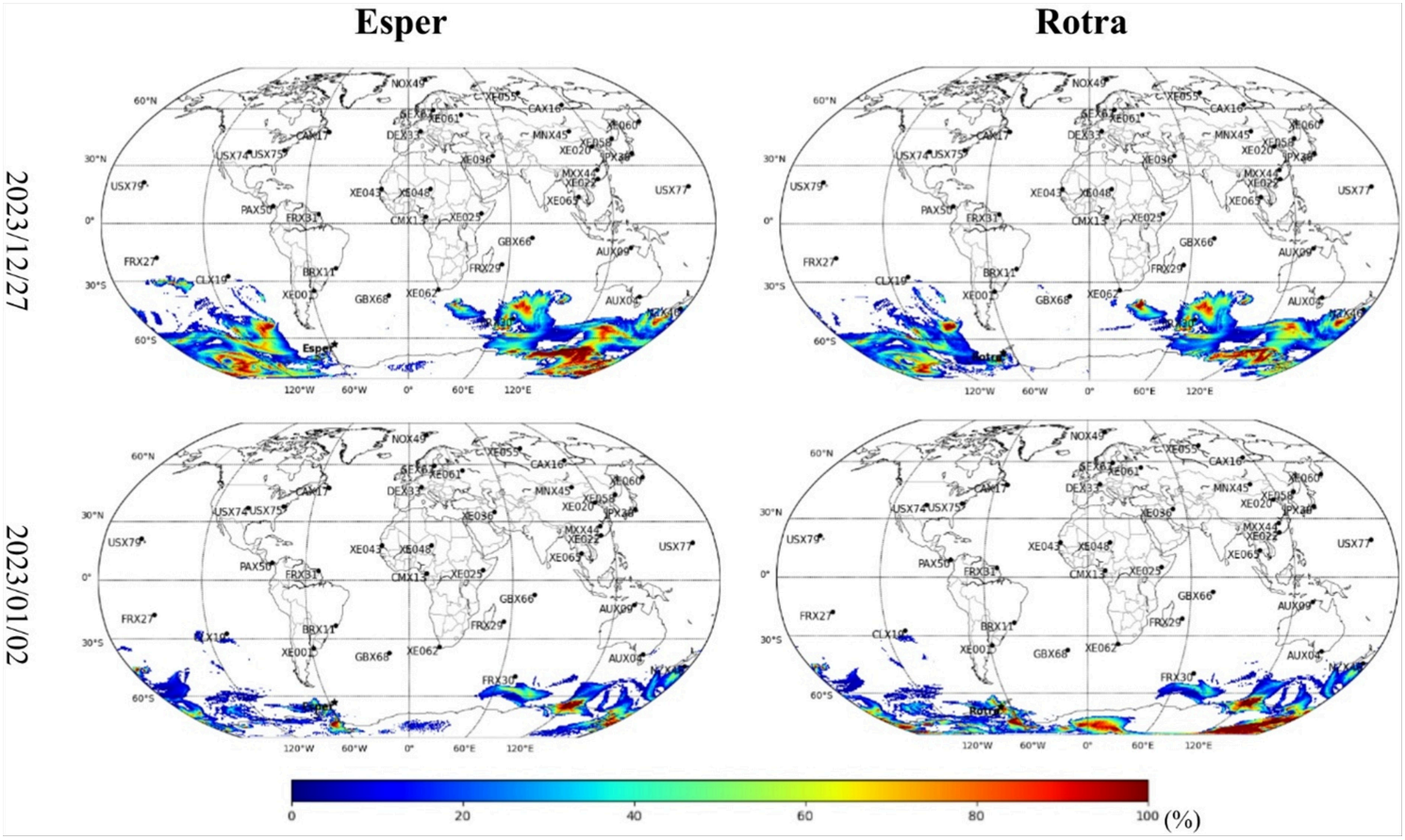


Figure 6

Effects of activating Esper (left column) and Rotra (right column) on NC, shown for December 27 (top row) and January 2 (bottom row).

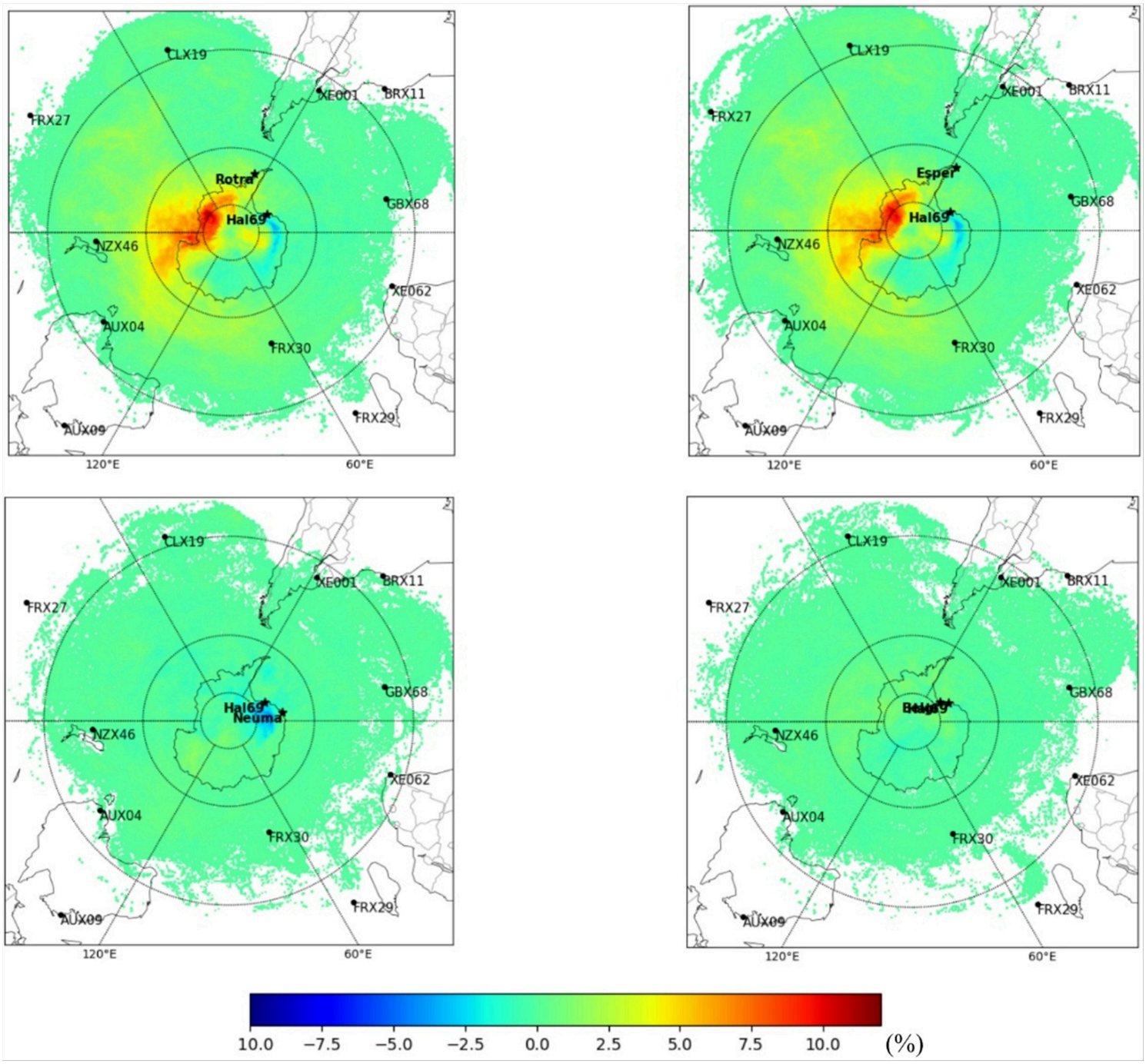


Figure 7

The mean yearly change in NC resulting from moving Hal69 to alternative sites is shown; the current station and proposed sites are indicated in bold and marked with a star.

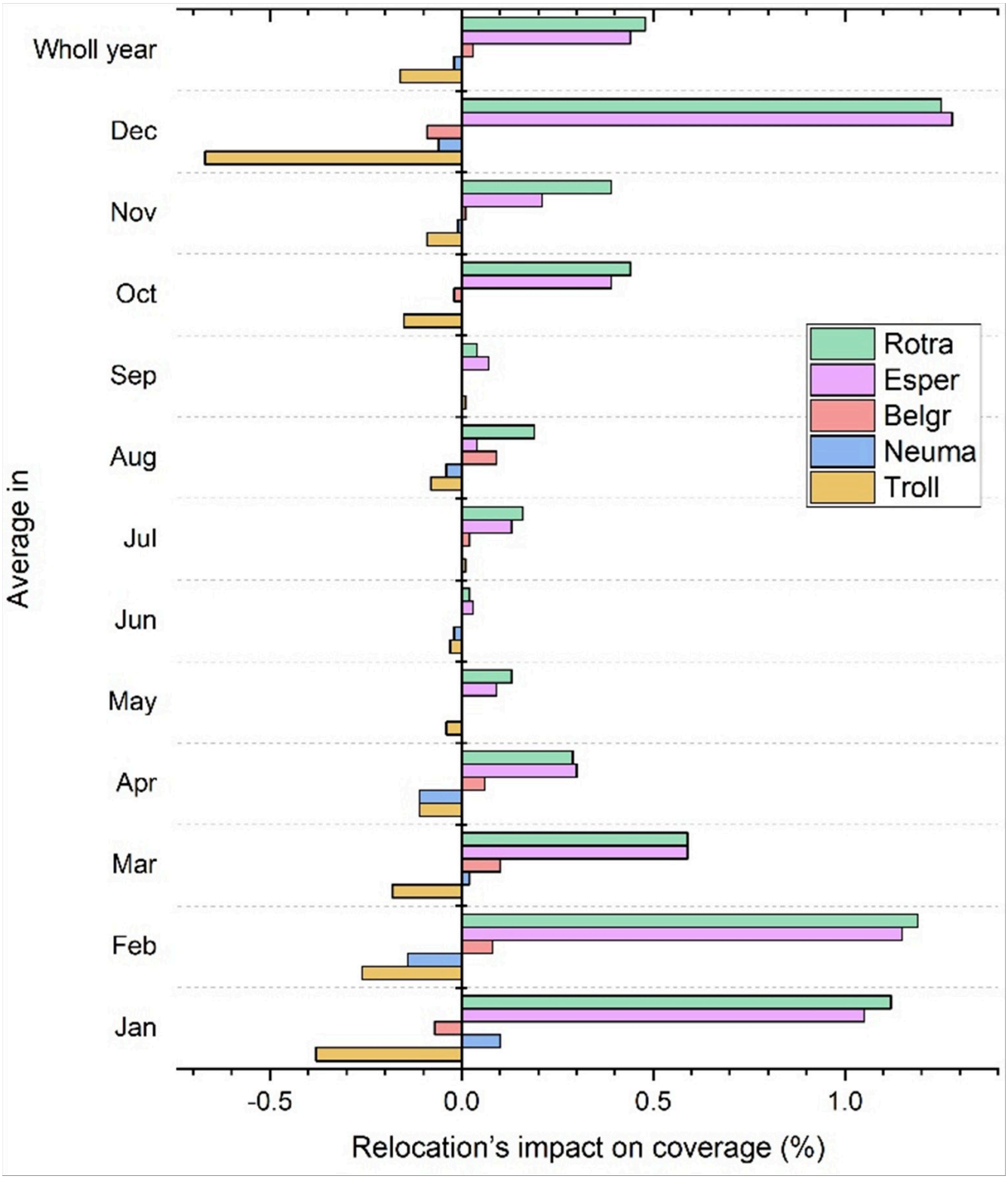


Figure 8

The monthly average impact of relocating the current station to Troll, Esper, Rotra, Neuma, and Belgr, color-coded as orange, purple, green, blue, and red.